Synthesis of flower-like and hexagonal flake-like ZnO using microwave method and their photocatalytic activity

Wei Si ✉, *Liran Pei*

School of Materials Science and Engineering, Dalian Jiaotong University, Dalian 116028, People's Republic of China
✉ *E-mail: siwei@djtu.edu.cn*

Published in Micro & Nano Letters; Received on 4th May 2020; Revised on 27th May 2020; Accepted on 10th June 2020

The flower-like and hexagonal flake-like ZnO microstructures were synthesised by a microwave method using ammonia water and sodium hydroxide as precipitant, respectively. The products were characterised by scanning electron microscopy, high-resolution transmission electron microscopy, X-ray diffraction and photoluminescence. The photocatalytic activity of the flower-like and hexagonal flake-like ZnO microstructures was evaluated by the degradation of methyl orange (MO) under ultraviolet (UV) light irradiation. The results indicated that the best flower-like ZnO microstructure was obtained when the experimental conditions were $[Zn^{2+}] = 0.025$ mol l^{-1}, $[Zn^{2+}]$:$[NH_3{\cdot}H_2O] = 1{:}1.5$, microwave power = 231 W. Under the same reaction conditions, hexagonal flake-like ZnO can be obtained by using sodium hydroxide as precipitant. The MO in aqueous solution was completely eliminated by flower-like ZnO after 120 min of UV light irradiation. Under identical conditions, the degradation of MO in aqueous solution was completely finished within 150 min in the presence of hexagonal flake-like ZnO. The flower-like ZnO sample showed an enhanced photocatalytic activity compared with the hexagonal flake-like ZnO for the MO degradation, which could be attributed to the presence of more active centres and hence can have more opportunities to contact with MO molecules.

1. Introduction: Microwave heating offers many advantages including rapid heating to crystallisation temperature, homogeneous nucleation and fast supersaturation by the rapid dissolution of precipitated hydroxides, which leads to lower crystallisation temperatures and shorter crystallisation times [1–3]. ZnO is a promising wide bandgap material that has gained considerable attention for the growth of nanostructures [4–6]. ZnO photocatalysts show relatively high activity [7–10], chemical stability and good properties [11–13] under ultraviolet (UV) light. Ivanov *et al.* [14] demonstrated a methodological approach for utilising microwave heating during the hydrothermal process to obtain highly dispersed ZnO crystals with high-photocatalytic activity. Li *et al.* [15] developed a fast and facile microwave and ultrasonic combined technique to fabricate well-defined flower-like ZnO nanostructures with a central petal and symmetrical six petals growing radially from the centre. Wu and Chen also have synthesised flower-like ZnO microstructure by a straightforward microwave–hydrothermal technique using zinc chloride and arginine solution as reactants.

The as-synthesised ZnO flowers exhibit a significant enhancement of photocatalytic capability towards degrading methyl blue (MB) under UV light, the photodegradation of MB reaches 95.60%, only within 2 h of adding the as-synthesised ZnO in the MB solution under UV irradiation [16]. The photoconducting ZnO film with a surface acoustic wave device has opened a potential market for a wireless UV light detector [17–19]. A variety of ZnO nanostructure morphologies, such as nanowires [20, 21], nanorods [22–25], nanosheets [26] and nanotubes have been synthesised [27, 28]. To the best of our knowledge, the synthesis of well-ordered flower-like ZnO nano-structures and microstructures in surfactant-free aqueous solution through simple microwave technique has not been reported. In the present work, we report a microwave method to prepare ZnO with novel three-dimensional (3D) morphology under mild conditions without the addition of any template, surfactant or metal catalyst.

2. Experimental: Zinc chloride ($ZnCl_2$), ammonia water ($NH_3{\cdot}H_2O$) and sodium hydroxide (NaOH) are used as starting materials. All chemicals are of analytical reagent. For flower-like ZnO, in a typical procedure, the ammonia water was added dropwise to $ZnCl_2$ aqueous solution ($[Zn^{2+}] = 0.025$ mol l^{-1}) with the material ratio of $[Zn^{2+}]$:$[NH_3{\cdot}H_2O] = 1{:}1.5$ under magnetic stirring for 3 min, and then treated in the microwave oven at power 231 W for 20 min. The settlings were collected by filtration and washed three times with anhydrous ethanol and distilled water in this order. The obtained sample was dried in a drying oven at 60°C for 6 h. To investigate the influence of reaction parameters on the morphologies of products, all concentration of Zn^{2+} (0.0125, 0.025 and 0.05 mol l^{-1}), material ratio (1:1, 1:1.5, 1:2), microwave irradiation time (10, 20 and 30 min) and microwave power (119, 231 and 385 W) were used while other experimental parameters were kept optimum conditions. The hexagonal flake-like ZnO was synthesised by mentioned typical procedure with sodium hydroxide as the precipitant.

Morphology of ZnO was characterised by a JSM-6360LV scanning electron microscopy (SEM) and a JEM-2100F high-resolution transmission electron microscopy (HRTEM). The crystal structure of ZnO was characterised by X-ray diffraction (XRD) using an Empyrean X-ray diffractometer with Cu Kα radiation. The room temperature photoluminescence (PL) was carried out on a Hitachi F-7000 fluorescence spectrophotometer using the 325 nm excitation line of 'Xe' light. The photocatalytic activity was investigated using methyl orange (MO) as a model organic dye on a UV–vis spectrometer 721. The optimum conditions were as follows: the 50 mg of the photocatalyst (ZnO) was dispersed in 100 ml the MO aqueous solution (10 mg/l). The solution has a depth of 1 cm and a pH of 7.0 (adjust pH value with the sodium hydroxide aqueous solution of 1 M). The UV light irradiation was carried out in a quartz dish using Xe lamp (25 W) at distant of 5 cm from the surface of the solution. Irradiation area was 490 cm^2, the temperature of the reaction was 30 °C. Before irradiation, the dye solution containing ZnO was stirred in the darkness for 30 min to get adsorption equilibrium. 1 ml of the solution was withdrawn at a regular interval time (10 min) and centrifuged. The efficiency of the degradation process was evaluated by monitoring the decolourisation rate of the dye near the maximum absorption wavelength ($\lambda_{MO} = 465$ nm) [2].

3. Results and discussion: Fig. 1 shows the SEM images of the prepared ZnO using ammonia water as the precipitant at different

© The Institution of Engineering and Technology 2020

concentration of Zn^{2+}. When the concentrations of Zn^{2+} were 0.0125, 0.025 and 0.05 mol l^{-1} (see Figs. 1*a*–*c*), the products prepared are mainly composed of flower-like microstructures assembled from microsheets with a diameter of about 1 μm.

Figs. 2*a* and *b* reveal that the morphology on increasing the material ratio and maintaining the remaining parameters displayed a distinct change. Fig. 2*a* shows that the ZnO nanorods with a length of about 320 nm, a diameter of about 80 nm and an aspect ratio of 4:1 were obtained when material ratio = 1:1. The flower-like ZnO was obtained with an increasing amount of ammonia water (Fig. 2*b*). Ammonia serves as the complex agent and forms zinc amino complex ($Zn(NH_3)_4^{2+}$) with zinc ion. Then, the hydrolysis of ammonia adjusts the pH of the reaction solution. Microwave appears to be particularly effective as a means of inducing nucleation and may affect the crystallisation, which is responsible for the formation of final flower-like ZnO

$$ZnCl_2 + 4NH_3 \times H_2O \xrightarrow{\text{microwave}} Zn(NH_3)_4^{2+} + 2Cl^- + 4H_2O \quad (1)$$

$$Zn(NH_3)_4^{2+} + 2OH^- \xrightarrow{\text{microwave}} ZnO + 4NH_3^- + H_2O \quad (2)$$

The change of microwave power has a great influence on the final morphology of ZnO (Figs. 2*c* and *d*). Compared with Fig. 1*b*, the best flower-like ZnO microstructure is obtained when

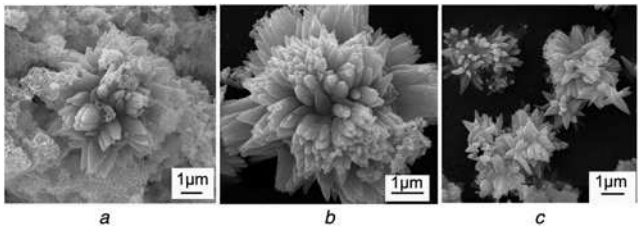

Fig. 1 *SEM images of the flower-like ZnO produced at different concentration of* Zn^{2+}
a 0.0125 mol l^{-1}
b 0.025 mol l^{-1}
c 0.05 mol l^{-1}

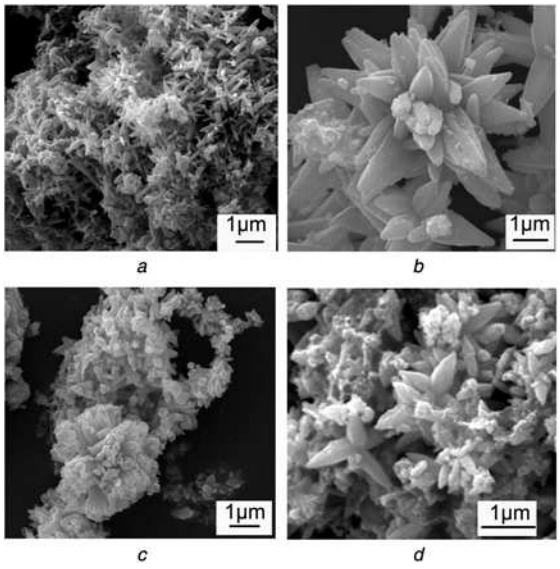

Fig. 2 *SEM images of the flower-like ZnO produced at different material ratio and microwave power*
a Material ratio = 1:1
b Material ratio = 1:2
c Microwave power = 119 W
d Microwave power = 385 W

the experiment conditions are $[Zn^{2+}] = 0.025$ mol l^{-1}, $[Zn^{2+}]$: $[NH_3 \cdot H_2O] = 1{:}1.5$ and microwave power = 231 W. The morphology of ZnO is a flower-like different from the hexagonal pyramid flower-like ZnO materials reported in other literatures, we prepared the flower-like ZnO is composed of self-assembly from a lot sharp angle sheet shape, with a very regular structure arrangement, similar to Chrysanthemum.

TEM, HRTEM and selected area electron diffraction (SAED) images of the best flower-like ZnO are presented in Fig. 3. The flower-like structure with a rachis radius of 100–150 nm can be observed in the TEM image in Fig. 3*a*. The lattice spacing was calculated to be 0.26 nm, corresponding to the distance the *d*-spacing of (002) crystal plane of the hexagonal ZnO (see Fig. 3*b*). The illustration in Fig. 3*b* suggests that these structures are polycrystalline.

Fig. 4 demonstrates under the above same reaction conditions, hexagonal flake-like ZnO with the side length of about 700 nm can be obtained by using sodium hydroxide as precipitant (illustration shows a local amplification of image). Here zinc cations are known to readily react with hydroxide anions to form stable Zn $(OH)_4^{2-}$ complexes, which act as the growth unit of ZnO microstructures [29]. Therefore, the growth mechanism of ZnO microstructures is considered as follows:

$$ZnCl_2 + 2NaOH \xrightarrow{\text{microwave}} Zn(OH)_2^- + 2NaCl \quad (3)$$

$$Zn(OH)_2 + 2H_2O \xrightarrow{\text{microwave}} Zn(OH)_4^{2-} + 2H^+ \xrightarrow{\text{microwave}} ZnO + 3H_2O \quad (4)$$

The XRD patterns of the flower-like and hexagonal flake-like ZnO are shown in Fig. 5, in which all diffraction peaks can be indexed to hexagonal ZnO (JCPDS 36–1451, $a = 3.249$ Å, $c = 5.206$ Å), no peaks other than ZnO are detected.

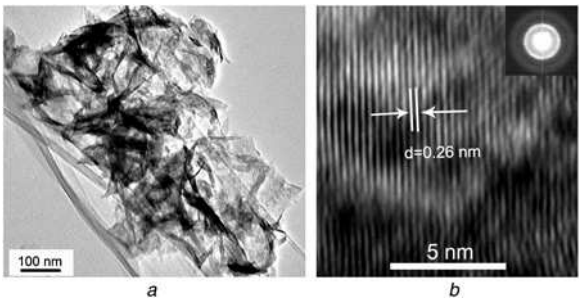

Fig. 3 *TEM, HRTEM with SAED pattern images of the flower-like ZnO*
a TEM image
b HRTEM image (SAED, see illustration)

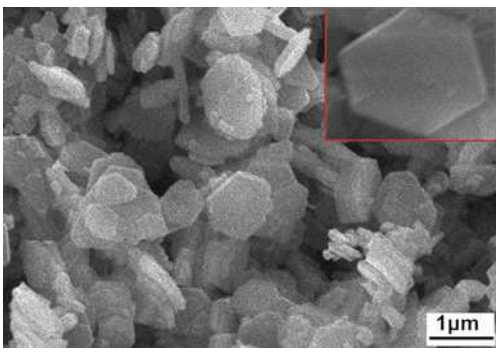

Fig. 4 *SEM images of the hexagonal flake-like ZnO*

© The Institution of Engineering and Technology 2020

doi: 10.1049/mnl.2020.0259

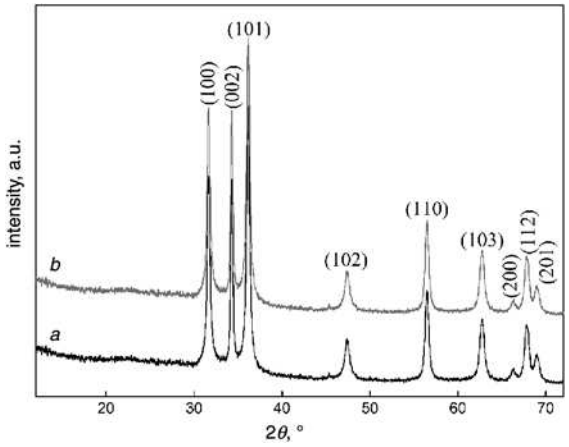

Fig. 5 *XRD patterns of the flower-like and hexagonal flake-like ZnO*
a Flower-like ZnO
b Hexagonal flake-like ZnO

The characteristic peaks have higher intensity, indicating the products have high purity and good crystallinity.

Based on the above results and related references [30], when the microwave power exceeds 200 W, the higher power microwave radiation shows a certain inhibitory effect on the growth of crystal nucleus, mainly the high energy microwave radiation reduces the probability of directional arrangement of confirmation ions on the lattice, which slows down the nucleation and growth process, thereby affecting the number of the photogenerated hole to a certain extent. In this experiment, the flower-like and hexagonal flake-like ZnO prepared under 231 W power was used to study the photocatalytic performance. The room temperature PL spectra are presented in Fig. 6.

Besides the peak located at about 470 nm, a broad emission peak in the range of 510–560 nm can be clearly observed. Compared to flower-like ZnO microstructures prepared using $NH_3{\cdot}H_2O$, the intensity of the emission peaks was weaker for hexagonal flake-like ZnO obtained using NaOH, indicating the optical properties of flower-like ZnO microstructure assembled from the microsheets are superior to others. The PL spectrum signal of the flower-like ZnO microstructure is stronger it may bring about quickening the recombination rate of electron and photogenerated hole caused by more surface defects and oxygen vacancies.

Fig. 7 presents the photocatalytic activities of the flower-like and hexagonal flake-like ZnO are evaluated by monitoring the decomposition of MO in aqueous solution under UV light irradiation.

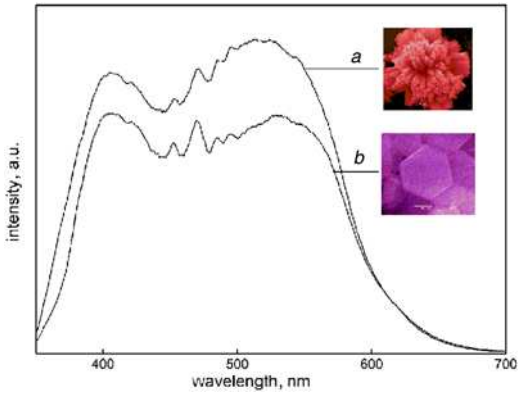

Fig. 6 *Room temperature PL spectra of the flower-like and hexagonal flake-like ZnO*
a Flower-like ZnO
b Hexagonal flake-like ZnO

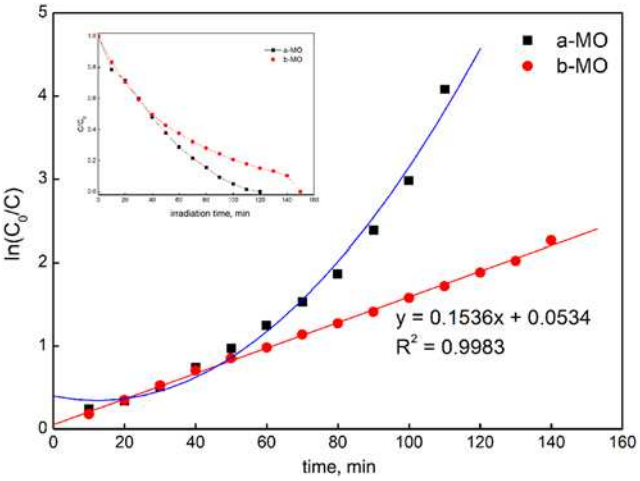

Fig. 7 *Photodegradation of MO using the flower-like and hexagonal flake-like ZnO as the photocatalyst, respectively*
a Flower-like ZnO
b Hexagonal flake-like ZnO

The MO in aqueous solution was completely eliminated by flower-like ZnO after 120 min UV light irradiation. Under identical conditions, the degradation of MO in aqueous solution was completely finished within 150 min in the presence of hexagonal flake-like ZnO (see illustration). The prepared flower-like ZnO is a regular shape formed by a perfect self-assembly process, which increases the number of active centres, and can have more opportunities to contact with MO molecules so that it can have better photocatalytic performance [31].

Further study on photocatalytic kinetics, the curves of $\ln(C_0/C)$ versus time demonstrates that the photodegradation reaction using the hexagonal flake-like ZnO as a photocatalyst is in correlation with the first-order rate equation. We estimated the rate constant (k) for our sample using the following equation $\ln(C_0/C) = kt$. The rate constant is 0.1536 min^{-1} for the hexagonal flake-like ZnO. Also, the square of the correlation coefficient is 0.9983. This shows a very good correlation. On the other hand, the curves of $\ln(C_0/C)$ versus time demonstrates that the photodegradation reaction using the flower-like ZnO as a photocatalyst is not in correlation with the first-order rate equation. The analysis indicates that it is not in correlation with the first and second rate equation and it needs further study.

A schematic diagram of the growing mechanism of the flower-like and hexagonal flake-like ZnO is shown in Fig. 8. The experimental results indicate that the microwave irradiation is mainly responsible to obtain the desired products. Microwave irradiation accelerates dramatically the reaction rate and shortens the reaction

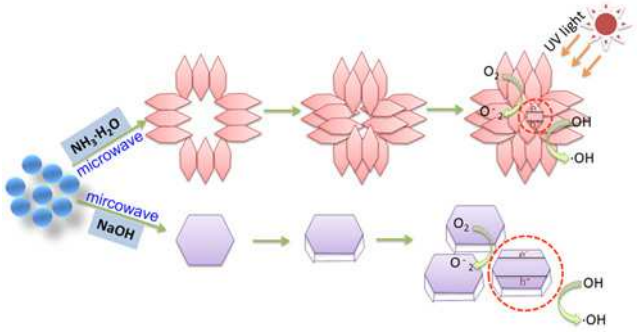

Fig. 8 *Schematic diagram of the growing mechanism of the flower-like and hexagonal flake-like ZnO*

© The Institution of Engineering and Technology 2020

time. It can promote the formation of perfect crystal nucleus, and then grow regular shape ZnO materials. When ZnO is irradiated with UV rays, the electrons in the valence band are excited to jump to the conduction band, generating photogenerated electrons and photogenerated holes. The photogenerated holes react with water adsorbed on the surface of ZnO to generate hydroxyl radicals (·OH), which can be effectively destroyed the molecular structure of MO adsorbed on the surface of ZnO and makes the MO fading.

4. Conclusion: The best flower-like ZnO microstructure was obtained when the experimental conditions were $[Zn^{2+}] = 0.025$ mol l^{-1}, $[Zn^{2+}]:[NH_3{\cdot}H_2O] = 1:1.5$ and microwave power = 231 W. Under the same reaction conditions, hexagonal flake-like ZnO can be obtained by using sodium hydroxide as precipitant. The role of the microwave was not only to accelerate the reaction between all the raw materials but also to lead to the growth and crystallisation of ZnO with 3D flower-like and hexagonal flake-like morphologies. The MO in aqueous solution was completely eliminated by hexagonal flake-like ZnO after 150 min UV light irradiation. Under identical conditions, the degradation of MO in aqueous solution was completely finished within 120 min in the presence of flower-like ZnO.

5. Acknowledgments: This work was supported by the Natural Science Foundation of Liaoning Province (20180550569), the Scientific Research Fund of Liaoning Provincial Education Department (JDL2019024) and the Program of Science-Technology Star for Young Scholars by the Dalian Municipality of China (2016RQ051).

6 References

[1] Li B., Wang Y.: 'Facile synthesis and enhanced photocatalytic performance of flower-like Zno hierarchical microstructures', *J. Phys. Chem. C*, 2010, **114**, (2), pp. 890–896

[2] Si W., Yu J.Y., Huang M.Y., *ET AL.*: 'Controllable synthesis and photocatalytic activities of cube and hexagonal prism ZnO', *Micro Nano Lett.*, 2012, **7**, pp. 1324–1327

[3] Shi R., Yang P., Dong X., *ET AL.*: 'Growth of flower-like ZnO on ZnO nanorod arrays created on zinc substrate through low- temperature hydrothermal synthesis', *Appl. Surf. Sci.*, 2013, **264**, pp. 162–170

[4] Callender R.H., Sussman S.S., Selders M., *ET AL.*: 'Dispersion of Raman cross section in CdS and ZnO over a wide energy range', *Phys. Rev. B*, 2015, **7**, (8), pp. 3788–3798

[5] Dutta M., Sarkar S., Ghosh T., *ET AL.*: 'Zno/graphene quantum dot solid-state solar cell', *J. Phys. Chem. C*, 2015, **116**, (38), pp. 20127–20131

[6] Horsthuis W.H.G.: 'Zno processing for integrated optic sensors', *Thin Solid Films*, 2017, **137**, (2), pp. 185–192

[7] He Y., Wang Y., Zhang L., *ET AL.*: 'High-efficiency conversion of CO_2 to fuel over ZnO/g-C3N4 photocatalyst', *Appl. Catalysis B Environ.*, 2015, **168–169**, (168), pp. 1–8

[8] Tsuji T., Terai Y., Kamarudin M.H.B., *ET AL.*: 'Photolumi-nescence properties of Sm-doped ZnO grown by sputtering-assisted metalorganic chemical vapor deposition', *J. Non-Cryst. Solids*, 2012, **358**, (17), pp. 2443–2445

[9] Mir L.E., Amlouk A., Barthou C., *ET AL.*: 'Synthesis and luminescence properties of $ZnO/Zn_2SiO_4/SiO_2$ composite based on nanosized zinc oxide-confined silica aerogels', *Phys. B Phys. Condensed Matter*, 2016, **388**, (1–2), pp. 412–417

[10] Wu J.M., Chen Y.R.: 'Ultraviolet-light-assisted formation of ZnO nanowires in ambient air: comparison of photoresponsive and photocatalytic activities in zinc hydroxide', *J. Phys. Chem. C*, 2011, **115**, (5), pp. 2235–2243

[11] Prasanna V.L., Vijayaraghavan R.: 'Insight into the mechanism of antibacterial activity of ZnO: surface defects mediated reactive oxygen species even in the dark', *Langmuir*, 2015, **31**, (33), pp. 9155–9162

[12] Arakha M., Saleem M., Mallick B.C., *ET AL.*: 'The effects of interfacial potential on antimicrobial propensity of ZnO nanoparticle', *Sci. Rep.*, 2015, **5**, pp. 1–10

[13] Murali A., Sarswat P, Sohn H.Y.: 'Enhanced photocatalytic activity and photocurrent properties of plasma- synthesized indium-doped zinc oxide nanopowder', *Mater. Today Chem.*, 2018, **11**, pp. 60–68

[14] Ivanov V.K., Shaporev A.S., Sharikov F.Y.: 'Baranchikov AY, hydrothermal and microwave-assisted synthesis of nanocrystalline Zno photocatalysts', *Superlattices Microstruct.*, 2007, **42**, pp. 421–424

[15] Li H., Liu E., Chan F.Y.F., *ET AL.*: 'Fabrication of ordered flower-like Zno nanostructures by a microwave and ultrasonic combined technique and their enhanced photocatalytic activity', *Mater. Lett.*, 2011, **65**, pp. 3440–3443

[16] Wu S.H., Jia Q.M., Sun Y.L., *ET AL.*: 'Microwave- hydrothermal preparation of flower-like ZnO microstructure and its photocatalytic activity', *Trans. Nonferrous Met. Soc.*, 2012, **22**, pp. 2465–2470

[17] Shankar S., Teng X., Li G., *ET AL.*: 'Preparation, characterization, and antimicrobial activity of gelatin/ZnO nano- composite films', *Food Hydrocolloids*, 2015, **45**, pp. 264–271

[18] Craciun V., Elders J., Gardeniers J.G.E., *ET AL.*: 'Growth of ZnO thin films on GaAs by pulsed laser deposition', *Thin Solid Films*, 2017, **259**, (1), pp. 1–4

[19] Abdelfattah N., Aakib H.E., Boukendil M., *ET AL.*: 'Controlling the structural properties of pure and aluminum doped zinc oxide nanoparticles by annealing', *J. King Saud Univ.-Sci.*, 2020, **32**, pp. 1074–1080

[20] Qin Y., Yang R., Wang Z.L.: 'Growth of horizonatal ZnO nanowire arrays on any substrate', *J. Phys. Chem. C*, 2015, **112**, (48), pp. 18734–18736

[21] Riaz M., Song J., Nur O., *ET AL.*: 'Study of the piezoelectric power generation of ZnO nanowire arrays grown by different methods', *Adv. Funct. Mater.*, 2015, **21**, (4), pp. 628–633

[22] Wu W., Hu G., Cui S., *ET AL.*: 'Epitaxy of vertical ZnO nanorod arrays on highly (001)-oriented ZnO seed monolayer by a hydrothermal route', *Cryst. Growth Des.*, 2016, **8**, (11), pp. 4014–4020

[23] Chang H., Sun Z., Ho K.Y., *ET AL.*: 'A highly sensitive ultraviolet sensor based on a facile in situ solution-grown ZnO nanorod/grapheme heterostructure', *Nanoscale*, 2011, **3**, pp. 258–264

[24] Gao S., Zhang H., Wang X., *ET AL.*: 'Zno-based hollow microspheres: biopolymer-assisted assemblies from ZnO nanorods', *J. Phys. Chem. B*, 2006, **110**, (32), pp. 15847–15852

[25] Mahmood K., Swain B.S., Amassian A.: '16.1% efficient hysteresis-free mesostructured perovskite solar cells based on synergistically improved ZnO nanorod arrays', *Adv. Energy. Mater.*, 2015, **5**, (17), pp. 1–11

[26] Qian H.S., Yu S.H., Gong J.Y., *ET AL.*: 'Growth of ZnO crystals with branched spindles and prismatic whiskers from $Zn_3(OH)_2V_2O_7{\cdot}H_2O$ nanosheets by a hydrothermal route', *Cryst. Growth Des.*, 2015, **5**, (3), pp. 935–939

[27] Ahmad M., Din R., Pan C., *ET AL.*: 'Investigation of hydrogen storage capabilities of ZnO-based nanostructures', *J. Phys. Chem. C*, 2015, **114**, (6), pp. 2560–2565

[28] Xu J., Chen Z., Zapien J.A., *ET AL.*: 'Surface engineering of ZnO nanostructures for semiconductor-sensitized solar cells', *Adv. Mater.*, 2015, **26**, (31), pp. 5337–5367

[29] Huang J., Xia C., Cao L., *ET AL.*: 'Facile microwave hydrothermal synthesis of zinc oxide one-dimensional nanostructure with three-dimensional morphology', *Mater. Sci. Eng., B*, 2008, **150**, pp. 187–193

[30] Liu X., Zhou Z.J., Zhang B.S, *ET AL.*: 'Effect of microwave treatment on structural changes and gasification reactivity of petroleum coke', *Ind. Eng. Chem. Res.*, 2011, **50**, (15), pp. 9063–9068

[31] Chen Z., Huang J., Wang Y., *ET AL.*: 'Controllable synthesis of Eu^{3+} ions doped Zn(OH)F and ZnO micro-structures: phase, morphology and luminescence property', *J. Rare Earths*, 2019, **37**, pp. 955–960

© The Institution of Engineering and Technology 2020

doi: 10.1049/mnl.2020.0259